The nonmevalonate pathway supports both monoterpene and sesquiterpene formation in snapdragon flowers

Natalia Dudareva*†, Susanna Andersson‡, Irina Orlova*, Nathalie Gatto‡, Michael Reichelt‡, David Rhodes*, Wilhelm Boland‡, and Jonathan Gershenzon‡

*Department of Horticulture and Landscape Architecture, Purdue University, West Lafayette, IN 47907; and ‡Max Planck Institute for Chemical Ecology, Beutenberg Campus, Hans-Knoell-Strasse 8, D-07745 Jena, Germany

Edited by Rodney B. Croteau, Washington State University, Pullman, WA, and approved December 1, 2004 (received for review October 4, 2004)

Terpenoids, the largest class of plant secondary metabolites, play essential roles in both plant and human life. In higher plants, the five-carbon building blocks of all terpenoids, isopentenyl diphosphate (IPP) and dimethylallyl diphosphate, are derived from two independent pathways localized in different cellular compartments. The methylerythritol phosphate (MEP or nonmevalonate) pathway, localized in the plastids, is thought to provide IPP and dimethylallyl diphosphate for hemiterpene, monoterpene, and diterpene biosynthesis, whereas the cytosol-localized mevalonate pathway provides C_5 units for sesquiterpene biosynthesis. Stable isotope-labeled, pathway-specific precursors (1-deoxy-[5,5-$^2H_2$]-D-xylulose and [2,2-$^2H_2$]-mevalolactone) were supplied to cut snapdragon flowers, which emit both monoterpenes and the sesquiterpene, nerolidol. We show that only one of the two pathways, the plastid-localized MEP pathway, is active in the formation of volatile terpenes. The MEP pathway provides IPP precursors for both plastidial monoterpene and cytosolic sesquiterpene biosynthesis in the epidermis of snapdragon petals. The trafficking of IPP occurs unidirectionally from the plastids to cytosol. The MEP pathway operates in a rhythmic manner controlled by the circadian clock, which determines the rhythmicity of terpenoid emission.

floral scent | terpenoids | volatiles | cross talk | mevalonic acid pathway

Isoprenoids, the largest family of natural products, play numerous vital roles in basic plant processes, including respiration, photosynthesis, growth, development, reproduction, defense, and adaptation to environmental conditions (1, 2). Plant-produced terpenoids also are essential nutrients in human diets and are used as chemotherapeutic agents with antitumor activities (3). Although isoprenoids are extraordinarily diverse, all originate through the condensation of the universal five-carbon precursors, isopentenyl diphosphate (IPP) and dimethylallyl diphosphate (DMAPP). In higher plants, two independent pathways located in separate intracellular compartments are involved in the biosynthesis of IPP and DMAPP. In the cytosol, IPP is derived from the classic mevalonic acid (MVA) pathway that starts from the condensation of acetyl-CoA (4, 5), whereas in plastids, IPP is formed from pyruvate and glyceraldehyde 3-phosphate via the methylerythritol phosphate (MEP or nonmevalonate) pathway (6–8). Initial research indicated that the cytosolic pool of IPP serves as a precursor of farnesyl diphosphate (FPP, C_{15}) and, ultimately, sesquiterpenes and triterpenes, whereas the plastidial pool of IPP provides the precursors of geranyl diphosphate (GPP, C_{10}) and geranylgeranyl diphosphate (GGPP, C_{20}) and, ultimately, monoterpenes, diterpenes, and tetraterpenes. However, cross talk between these two different IPP biosynthetic pathways has been documented (9–14), and the relative contributions of each pathway to the biosynthesis of the various classes of terpenes remain uncertain.

Terpenoids emitted from snapdragon flowers (*Antirrhinum majus*) include three monoterpenes, myrcene, (*E*)-β-ocimene, and linalool, derived from GPP, and a sesquiterpene, nerolidol, derived from farnesyl diphosphate. Emission of these compounds follows diurnal rhythms and is controlled by a circadian clock (15). The presence of monoterpenes and a sesquiterpene in a single mixture allowed us to examine the possible interactions between the two IPP biosynthetic pathways. By using stable isotope-labeled, pathway-specific precursors supplied to cut snapdragon flowers, we show that only one of the two pathways, the plastid-localized MEP pathway, provides IPP precursors for both plastidial monoterpene and cytosolic sesquiterpene biosynthesis. The MEP pathway operates in a rhythmic manner controlled by the circadian clock and determines the rhythmicity of terpenoid emission. The trafficking of IPP occurs unidirectionally from the plastids to cytosol.

Materials and Methods

Plant Material, Chemicals, and Stable Isotope-Labeled Compounds. Snapdragon (*A. majus*) Maryland True Pink cv. (Ball Seed, West Chicago, IL) was grown under standard greenhouse conditions as described in ref. 16. The pathway-specific inhibitors fosmidomycin and mevinolin were purchased from Molecular Probes and Sigma, respectively. Before use, the lactone of mevinolin was converted to the open acid form as described in ref. 17. Pathway-specific precursor 1-deoxy-[5,5-$^2H_2$]-D-xylulose ([$^2H_2$]-DOX) was synthesized from commercially available 2,3-*O*-isopropylidene-D-tartrate as described in refs. 18 and 19. Racemic [2,2-$^2H_2$]-mevalolactone ([$^2H_2$]-MVL) was prepared from commercially available unlabeled *rac*-mevaloactone by proton exchange. Commercial mevalolactone (0.13 g, 1 mM) was dissolved in deuterated methanol (CH_3O^2H, 5 ml) and treated with 1,5-diazabicyclo[3.4.0]non-5-ene (10 μl, 0.08 mM) to catalyze the isotope exchange. After stirring for 24 h at room temperature, the solvent was removed in vacuum and the product was purified by chromatography on silica gel by using ether:methanol (20:1, vol/vol) for elution. According to ^{1}H NMR and MS, the product consisted of [2,2-$^2H_2$]-MVL (>98% ^{2}H) and ≈30% of the acyclic methyl ester of [2,2-$^2H_2$]-mevalonic acid (>98% ^{2}H). Because mevalolactone easily passes membranes and is readily opened in the plant cell to give mevalonic acid, the lactone [$^2H_2$]-MVL was used for feeding experiments.

Labeling Experiments and Volatile Analysis. All labeling experiments were performed in a growth chamber under conditions of

This paper was submitted directly (Track II) to the PNAS office.

Abbreviations: IPP, isopentenyl diphosphate; DMAPP, dimethylallyl diphosphate; MVA, mevalonic acid; MVL, racemic [2,2-$^2H_2$]-mevalolactone; MEP, methylerythritol phosphate; GPP, geranyl diphosphate; DOX, 1-deoxy-D-xylulose; DXP, 1-deoxy-D-xylulose-5-phosphate; DXPS, DXP synthase; DXR, 1-deoxy-D-xylulose-5-phosphate reductoisomerase; HMGR, 3-hydroxy-3-methylglutaryl-CoA reductase; amu, atomic mass units.

Data deposition: The sequences reported in this paper have been deposited in the GenBank database [accession nos. AY770406 (for snapdragon *DXR* gene) and AY770407 (for snapdragon *DXPS* gene)].

†To whom correspondence should be addressed. E-mail: dudareva@hort.purdue.edu.

PLANT BIOLOGY

21°C, 50% relative humidity, 150 μmol·m^{-2}·s^{-1} light intensity, and a 12-h photoperiod. Although emission of floral volatiles from snapdragon flowers is developmentally regulated, 5- to 8-day-old flowers emit very similar amounts of volatiles (15, 16). Thus, to minimize the effect of developmental regulation, 5-day-old flowers were cut from the plants and transferred to small glass beakers (three flowers per beaker) filled with 10 ml of 5% (wt/vol) sucrose in tap water (control). For feeding experiments, [$^2H_2$]-DOX and [$^2H_2$]-MVL were supplied to 5% (wt/vol) sucrose at concentrations of 2 mg/ml and 3 mg/ml, respectively. For inhibition experiments, either fosmidomycin or mevinolin was added to 5% (wt/vol) sucrose to a final concentration of 100 μM. The chosen concentrations of inhibitors had no effect on flower appearance for the duration of the experiments. Emitted volatiles were collected by a closed-loop stripping method (20) every 3 h for 60 h under normal light/dark conditions (12-h photoperiod) and for 81 h under constant dark conditions. Volatiles were eluted from Porapak Q traps (80/100 mesh size; Alltech Associates) with 200 μl of CH_2Cl_2, and 2 μg of nonyl acetate was added as an internal standard. The amount and isotope abundance of emitted terpenoids were analyzed by GC-MS on a Hewlett–Packard 6890 gas chromatograph (injector temperature 220°C and splitless injection with volume of 1 μl) coupled to a Hewlett–Packard 5973 quadrupole mass selective detector. Separation was performed on a DB-5MS column (30 m $\times$ 0.25 mm $\times$ 0.25 μm film; Agilent Technologies, Böblingen, Germany) with helium as the carrier gas. The temperature program was as follows: initial oven temperature of 40°C for 3 min, increased at 5°C/min to 120°C, followed by an increase of 10°C/min to 180°C and final heating of the column at 300°C for 3 min. GC-MS was performed with a transfer-line temperature of 230°C, a source temperature of 230°C, a quadrupole temperature of 150°C, an ionization potential of 70 electron volts, and a scan range of m/z from 50 to 300. For quantification, representative selected ion peaks of each compound were integrated and the amounts were calculated in relation to the response of the internal standard at a m/z of 69. Response curves for the quantified compounds relative to the internal standard were generated by injecting a mixture of equal amounts of commercial standards (all from Fluka, except nerolidol, which was from Sigma) and the internal standard onto the GC-MS. The percentage of labeling was determined as the intensity of the shifted representative fragment ion (i.e., for myrcene m/z 95 or 97) divided by the sum of intensities for unshifted and shifted representative fragment ions (i.e., for myrcene m/z 93, 95, or 97). Two to three independent feeding experiments were performed, each containing duplicate samples.

RNA Isolation and RNA Gel Blot Analysis. Total RNA from snapdragon floral tissues and petals at nine time points during a daily light/dark cycle was isolated and analyzed as described in refs. 15 and 21. A 2.57-kb *Eco*RI/*Xho*I fragment containing the coding region of the DXPS gene (clone S_1_1_N11 from snapdragon petal-specific EST collection; GenBank accession no. AY770407), a 1.42-kb PCR fragment containing the DXR gene coding region (GenBank accession no. AY770406), and a 0.5-kb fragment containing the coding region of the HMGR gene obtained by means of RT-PCR with (forward) 5′-TTGAGTTCCACCCCAACTGTAC-3′ and (reverse) 5′-CTTGATGCAATGGGGATGAACA-3′ primers were used as probes in RNA gel blot analyses. Five micrograms of total RNA was loaded in each lane. The blots were rehybridized with 18S rDNA for loading control.

Results and Discussion

Monoterpene and Sesquiterpene Biosynthesis in Snapdragon Petals Involves only the MEP Pathway. To determine the involvement of the two IPP pathways in the biosynthesis of monoterpene and sesquiterpene compounds of floral scent, cut snapdragon flowers were treated with fosmidomycin (100 μM in 5% sucrose), a specific inhibitor of the first committed enzyme of the plastidial MEP pathway, 1-deoxy-D-xylulose-5-phosphate reductoisomerase (DXR) (22), and floral scent was collected by closed-loop stripping (20) every 3 h for 60 h under normal light/dark conditions (12-h photoperiod). Both monoterpene and sesquiterpene emissions were confined principally to the light period. Fosmidomycin inhibited not only monoterpene emission, which declined by 60% in the first 3 h after treatment, compared with control flowers fed only with sucrose solution (Fig. 1*A*), but also nerolidol emission (Fig. 1*B*), although the effect was not as rapid as that of monoterpene compounds. (The results for all of the monoterpene compounds were similar, so data are presented only for one representative, myrcene.) These results indicate that the MEP pathway provides a major IPP and DMAPP source for

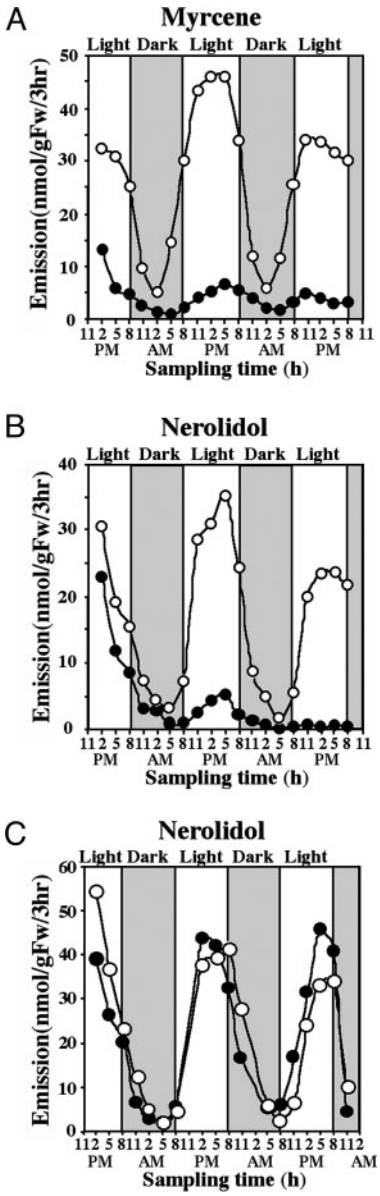

Fig. 1. Effect of fosmidomycin (*A* and *B*) and mevinolin (*C*) on myrcene and nerolidol emission. Filled circles represent emission from fosmidomycin-treated or mevinolin-treated flowers, and open circles represent control flowers fed with sucrose solution. Mevinolin had no effect on the emission of nerolidol (*C*) or myrcene (data not shown).

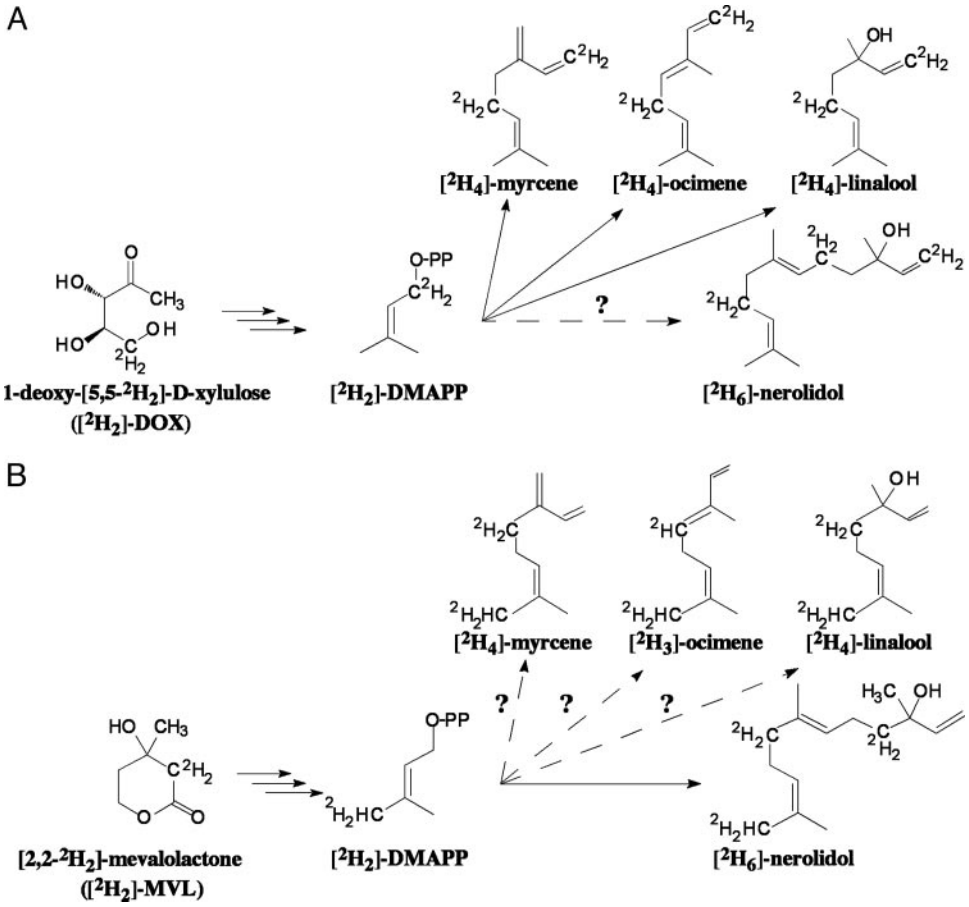

Fig. 2. Potential labeling patterns of monoterpenes and nerolidol by $[^2H_2]$-DOX (*A*) and $[^2H_2]$-MVL (*B*).

both monoterpene and sesquiterpene biosynthesis in snapdragon flowers. Because the synthesis of sesquiterpenes takes place in the cytosol, there must be an export of isoprenoid intermediates from the plastids to the cytosol. Consistent with these data, mevinolin (100 μM in 5% sucrose), a specific inhibitor of the key enzyme of the MVA pathway, 3-hydroxy-3-methylglutaryl-CoA reductase (HMGR) (23), had virtually no effect on the amount of emitted nerolidol (Fig. 1*C*), suggesting that the MVA pathway does not contribute to nerolidol production in snapdragon flowers.

To confirm the involvement of the MEP pathway in nerolidol biosynthesis, cut snapdragon flowers were supplied with the dephosphorylated form of the first intermediate of the pathway, $[^2H_2]$-DOX (2 mg/ml in 5% sucrose) (Fig. 2*A*), and the amount and isotope abundance of emitted terpenoids were analyzed by GC-MS every 3 h for 60 h. Exogenously supplied $[^2H_2]$-DOX did not affect the total amount of monoterpenes or nerolidol emitted, compared with control flowers fed with sucrose (Fig. 3 *A* and *B*), indicating that flux through the pathways did not increase in these experiments, although substantial labeling was observed. Labeled monoterpene isotopomers were easily distinguished from unlabeled compounds by a shift of +2 atomic mass units (amu) when either labeled IPP or DMAPP was used for GPP biosynthesis and +4 amu when IPP and DMAPP were both labeled (Fig. 2*A*). Surprisingly, the level of $[^2H_2]$-DOX labeling was greater at night than during the day, with the differences being more profound for labeling by 4 amu. At night, monoterpene enrichment by 4 amu was 7.5-fold (in myrcene) (Fig. 3*A Right*) to 17-fold (in ocimene) higher than during the day. These differences may be a consequence of the rhythmic operation of the endogenous MEP pathway, with greater flux during the light period reducing the incorporation of exogenous substrates.

The sesquiterpene, nerolidol, also became labeled by $[^2H_2]$-DOX in these experiments, and its newly synthesized labeled isotopomers exhibited a shift of not only +2 and +4 amu, but also of +6 amu (Fig. 3*B Right*), because two IPP molecules and one DMAPP are required for its biosynthesis. Similar to monoterpenes, the level of nerolidol labeling changes rhythmically in these experiments, with a maximum during the night and a minimum during the day (Fig. 3*B Right*). The labeling of nerolidol by +6 amu in $[^2H_2]$-DOX feeding experiments provides indirect evidence that IPP and/or DMAPP are the plastid intermediates exported to the cytosol, because the export of plastidial GPP (which could then condense with cytosolic IPP) would lead to a maximum labeling of nerolidol of only +4 amu.

Rhythmicity in Flux Through the MEP Pathway Is Controlled by a Circadian Clock and Rhythmic Gene Expression. Because the two immediate precursors of the MEP pathway, pyruvate and glyceraldehyde 3-phosphate, may be derived directly from the Calvin cycle, the rhythmic changes in the flux through the pathway could be either induced by light or controlled by an endogenous clock. To determine the light-dependency of this pathway in snapdragon flowers, cut flowers were transferred to continuous dark and fed with $[^2H_2]$-DOX, and floral scent was collected every 3 h for 81 h. The oscillations in emission and the levels of labeling of myrcene and nerolidol continued under free-running conditions, indicating that the flux through the MEP pathway in snapdragon flowers follows a diurnal rhythm that is controlled by a circadian clock (Fig. 3*C*). The diurnal fluctuations com-

PLANT BIOLOGY

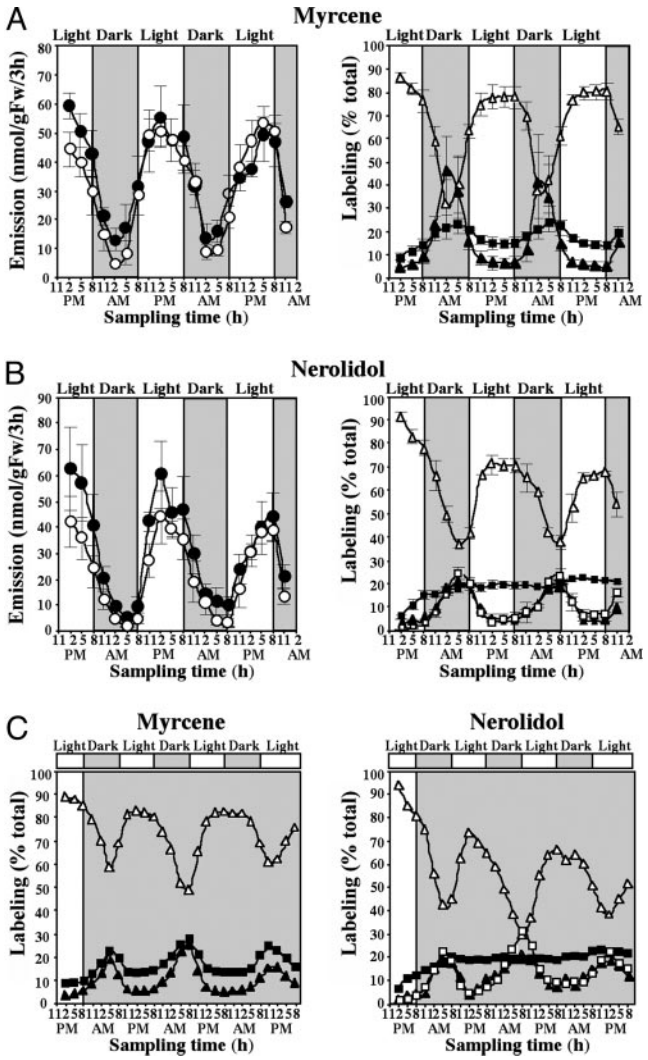

Fig. 3. Emission and *in vivo* labeling kinetics of myrcene (*A*) and nerolidol (*B*) during feeding of snapdragon flowers with [$^2H_2$]-DOX under normal dark/light conditions. Filled and open circles (*Left*) represent total emission from [$^2H_2$]-DOX-fed and control (only fed with sucrose solution) flowers, respectively. Open triangles (*Right*) represent percent of unlabeled compounds emitted, and filled squares and triangles represent percent of myrcene and nerolidol labeled by +2 and +4 amu, respectively; open squares represent percent of nerolidol labeled by +6 amu. (*C*) *In vivo* labeling of myrcene and nerolidol during feeding of snapdragon flowers with [$^2H_2$]-DOX in constant dark.

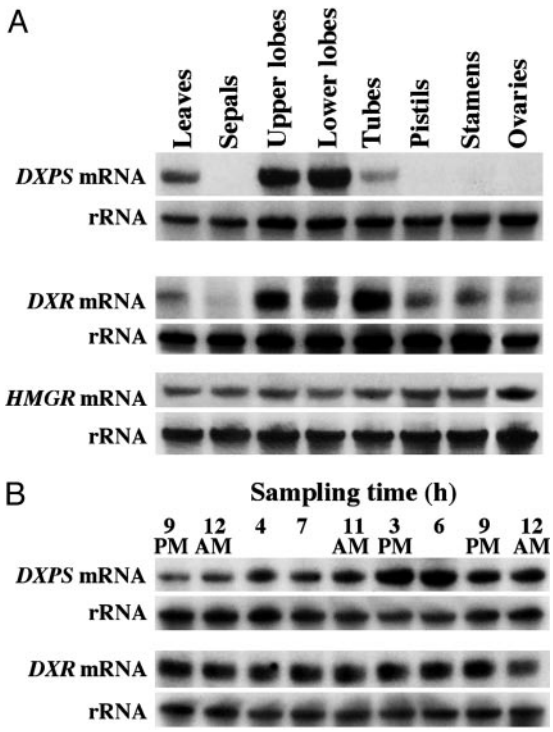

Fig. 4. Expression of DXPS, DXR, and HMGR genes in leaves and different floral tissues of snapdragon flowers. (*A*) *DXPS* and *DXR* mRNA expression in snapdragon petals during a normal light/dark cycle. (*B*) RNA blots were rehybridized with an 18S rDNA probe to control for differences in sample loading.

monly observed in the emission of a variety of other plant terpenoids, such as isoprene (24) and herbivore-induced monoterpenes and sesquiterpenes (25), also are likely to be a result of this rhythmicity in the MEP pathway. The absence of a direct light effect on terpene emission in snapdragon is consistent with the fact that both biosynthesis and emission occur in the conical cells of the petal epidermis, which are nonphotosynthetic (26).

Previous analysis of the expression of monoterpene synthase genes responsible for the formation of myrcene and ocimene in snapdragon flowers during a light/dark cycle revealed only a weak diurnal oscillation pattern despite the strong difference in light vs. dark emission rates (15). These data suggest that the activities of upstream enzymes in monoterpene formation could lead to the rhythmic emission of monoterpene compounds. The first step of the MEP pathway is the condensation of pyruvate and glyceraldehyde 3-phosphate to form 1-deoxy-D-xylulose-5-phosphate (DXP) catalyzed by the transketolase DXP synthase (DXPS). DXP, in turn, is converted to methylerythritol phosphate by DXR. Although DXPS is thought to be an important rate-controlling step of the MEP pathway (27), DXR also may serve as a significant control point, because it is the first committed step of the MEP pathway of terpenoid biosynthesis (28). DXP is a precursor for the synthesis of thiamin and pyridoxol (29, 30) as well as IPP and DMAPP. Thus, we investigated both DXPS and DXR gene expression in leaves and different floral tissues of snapdragon. The DXPS gene was highly expressed in leaves and in upper and lower petal lobes, the parts of the flower that were previously shown to be primarily responsible for terpenoid production and emission in snapdragon (15). The DXR gene was expressed in all tissues examined except sepals but with preferential expression in those tissues that are involved in volatile biosynthesis (Fig. 4*A*). When the accumulation of *DXPS* and *DXR* mRNA was examined in upper and lower petal lobes at nine time points during a 27-h interval by RNA gel blot analysis, the level of DXPS, but not DXR, transcripts showed a diurnal oscillation pattern increasing during the light period, with a maximum accumulation around 3–6 p.m. (Fig. 4*B*), strongly correlating with the pattern of monoterpene and nerolidol emissions (Fig. 1). These results suggest that DXPS determines the tissue-specificity and rhythmic pattern of the MEP pathway, although some additional regulation also takes place downstream of DXPS, because exogenously supplied [$^2H_2$]-DOX (converted to DXP *in planta*) does not significantly alter terpene emission patterns (Fig. 3 *A Left* and *B Left*). The lack of diurnal oscillations in DXR transcript levels could be due to a minor role of DXR in the regulation of the MEP pathway in snapdragon or posttranscriptional regulation of DXR activity. Additionally, the generic DXR probe used in these experiments could have recognized

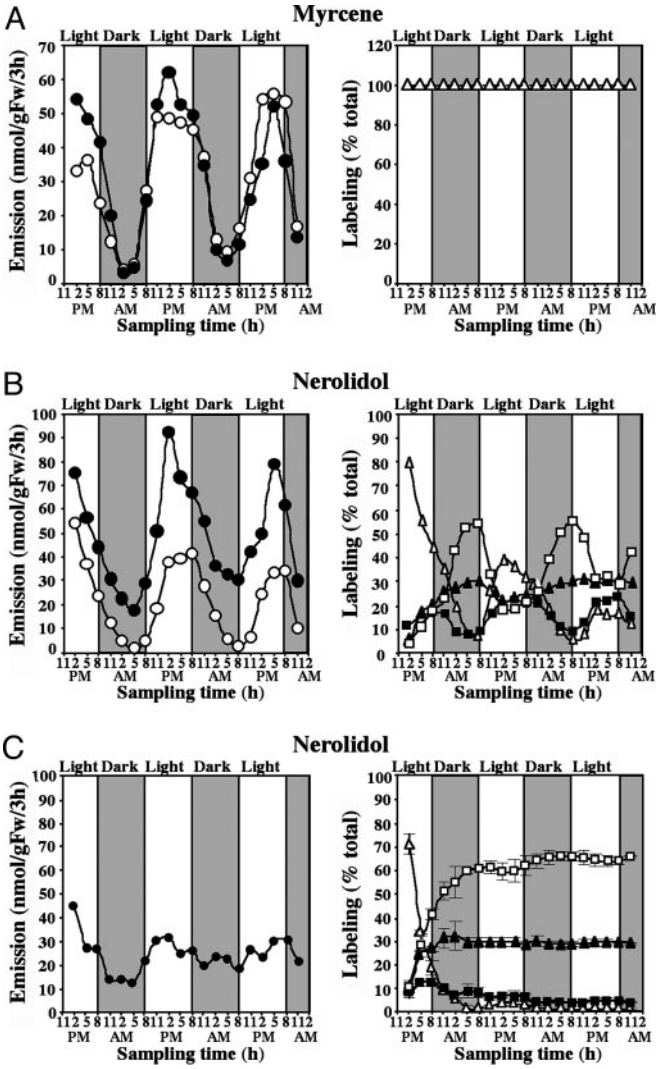

Fig. 5. Emission and *in vivo* labeling kinetics of myrcene (*A*) and nerolidol (*B* and *C*) during feeding of snapdragon flowers with $[^2H_2]$-MVL (*A* and *B*) and $[^2H_2]$-MVL/fosmidomycin (*C*). Filled circles represent emission from $[^2H_2]$-MVL fed or $[^2H_2]$-MVL/fosmidomycin-fed flowers, and open circles represent control flowers fed with sucrose solution. Open triangles represent percent of unlabeled compounds, and filled squares and triangles represent percent of myrcene and nerolidol labeled by +2 and +4 amu, respectively; open squares represent percent of nerolidol labeled by +6 amu.

more than one possible DXR isoform and so masked the correlation of expression of a specific DXR isogene with monoterpene and sesquiterpene emission.

MVA Pathway in Snapdragon Flowers Is Blocked at HMGR. The fosmidomycin and mevinolin inhibition data, combined with the $[^2H_2]$-DOX labeling experiments described above, suggest that monoterpene and sesquiterpene biosynthesis in snapdragon flowers relies on the plastidial supply of IPP and DMAPP via the MEP pathway. To determine the contribution of the MVA pathway, if any, $[^2H_2]$-MVL (3 mg/ml in 5% sucrose) (Fig. 2*B*) was supplied to cut snapdragon flowers, and floral scent was collected every 3 h for 60 h under normal light/dark conditions (12-h photoperiod). The exogenously supplied $[^2H_2]$-MVL had no effect on the level of emitted monoterpenes (Fig. 5*A Left*) but surprisingly led to a 2.4- and 10-fold increase in nerolidol emission during the day and night, respectively, compared with either control flowers fed only with a sucrose solution (Fig. 5*B Left*) or with flowers supplied with $[^2H_2]$-DOX (Fig. 3*B Left*). This increase in nerolidol emission suggests that the level of emitted nerolidol is limited by the level of precursors from the terpenoid pathway. Although there was no detectable incorporation of $[^2H_2]$-MVL into monoterpenes (Fig. 5*A Right*), nerolidol was efficiently labeled by $[^2H_2]$-MVL, with its maximum at night and its minimum during the day (Fig. 5*B Right*). When the contribution of the MEP pathway to nerolidol production was eliminated by treatment with fosmidomycin, the rhythmicity in nerolidol emission completely disappeared, and $[^2H_2]$-MVL feeding led to an almost complete deuterium labeling of nerolidol (Fig. 5*C*). Hence, in the absence of the MEP pathway, nerolidol production is observed via the MVA pathway but only in the presence of exogenous mevalonate. The endogenous MVA pathway thus does not contribute to nerolidol production in snapdragon flowers and is blocked before mevalonic acid even though the later enzymes of the pathway are active. Analysis of HMGR gene expression in leaves and all floral tissues revealed that the HMGR gene was expressed constitutively in all tissues examined but at very low levels (transcripts became visible only after 10 days exposure of filter to film) (Fig. 4*A*). An additional confirmation of low HMGR gene expression is that the sequence of this gene was not found a single time during an extensive search of 10,000 nonredundant ESTs from a normalized snapdragon cDNA library constructed by using mRNAs isolated from roots, seedlings, young and old vegetative apices, influorescences, young buds and flowers at different developmental stages, and both fertilized and unfertilized carpels. The low level of HMGR gene expression, along with the ineffectiveness of mevinolin treatment (Fig. 1*C*) and the facile incorporation of exogenous mevalonate into sesquiterpene end products, leads us to surmise that the MVA pathway is blocked at HMGR.

Cross Talk Between Cytosolic and Plastidial Pathways of Isoprenoid Biosynthesis Occurs Unidirectionally from Plastids to Cytosol. Much research on plant terpene biosynthesis has focused on the cross talk between the two pathways. Recent analysis of changes in metabolite pools mediated by MVA and MEP pathway-specific inhibitors provided indirect evidence for the unidirectional transport of isoprenoid intermediates from the plastids to the cytosol in *Arabidopsis thaliana* seedlings (13). Our results on the incorporation of $[^2H_2]$-DOX into the sesquiterpene nerolidol (Fig. 3*B*), along with the lack of detectable incorporation of $[^2H_2]$-MVL into monoterpenes (Fig. 5*A*), provide clear evidence of cross talk in snapdragon flowers between the two IPP biosynthetic pathways that occurs unidirectionally from the plastids to the cytoplasm. Such trafficking of isoprenoid intermediates could be mediated by a specific metabolite transporter, which was recently characterized in spinach (31). The transport of intermediates from the plastidial MEP pathway to the cytosol competes with the flux to GPP, the precursor of monoterpenes. Although both fluxes depend on plastidial IPP concentration, transport flux has a linear dependence on IPP, whereas flux to GPP depends on the square of IPP concentration and thus is more sensitive to IPP pool size than the competing transport flux. This fact could explain the observation that fosmidomycin blocks monoterpene emission before affecting nerolidol (Fig. 1 *A* and *B*). When snapdragon flowers were fed with $[^2H_2]$-DOX, the peak of nerolidol labeling occurred later in the diurnal cycle (5–8 a.m.) (Fig. 3*B Right*) than did the peak of myrcene labeling (2 a.m.) (Fig. 3*A Right*), which suggests that there is some delay in substrate supply for nerolidol formation.

The discovery that plant isoprenoids are formed by two independent pathways ranks as one of the most important achievements of plant biochemistry in the last decade. Here, we show that only one of the two pathways is operating in the formation of volatiles isoprenoids in snapdragon petals. The MEP pathway, localized in the plastids, provides IPP and

DMAPP precursors for both monoterpene biosynthesis (in plastids) and sesquiterpene biosynthesis (in the cytosol) and determines their rhythmic emission. On the other hand, the MVA pathway, localized in the cytosol, appears to be inactive in the petal tissue of open flowers. The down-regulation of one of the two isoprenoid pathways under particular environmental or developmental conditions (32) or in specific cell types may well be an important hallmark of plant metabolism. In *Arabidopsis* seedlings, the MVA pathway is down-regulated in light (32). The present study examined snapdragon petals, which form volatile terpenes only in the epidermis, which is nonphotosynthetic. In the secretory cells of peppermint glandular trichomes, another nonphotosynthetic cell type important in terpene biosynthesis, there are indications that the MVA pathway also is blocked at HMGR. A study undertaken before the MEP pathway was discovered demonstrated that both monoterpene and sesquiterpene biosynthesis rely exclusively on a plastid-derived IPP pool (33). Similar to snapdragon flowers (Fig. 5*B Left*), [^{14}C] mevalonic acid feeding to the isolated peppermint secretory cells led to a substantial increase in sesquiterpene formation. But, in contrast to snapdragon (Fig. 5*A Right*), the incorporation of radioactive precursor was found in both monoterpenes and sesquiterpenes (33).

The cooccurrence of two completely distinct pathways for isoprenoid formation in plant cells is remarkable because a similar situation does not hold for any other major metabolic route. The plastidial pathway probably arose from genes contained in a cyanobacterium-like symbiont that served as the progenitor of modern chloroplasts, although lateral gene transfer from eubacteria also may have occurred (34, 35). However, this scenario still does not explain the persistence of both pathways in contemporary plants. The answer may lie in the enormous variety of isoprenoids formed by plants, which could require two separate pathways composed of completely different enzymes and different intermediates to facilitate separate regulation. Further study of when and where the two pathways are active in plants should shed further light on questions regarding their evolutionary origin and maintenance.

This work was supported by National Science Foundation Grant MCB-0212802 (to N.D.), the Fred Gloeckner Foundation, the German Academic Exchange Service (N.D.), and the Max Planck Society (J.G.). This paper is contribution no. 17456 from the Purdue University Agricultural Experiment Station (West Lafayette, IN).

1. Gershenzon, J. & Kreis, W. (1999) in *Biochemistry of Plant Secondary Metabolism*, ed. Wink, M. (CRC, Boca Raton, FL), pp. 222–299.
2. Rodriguez-Concepcion, M. & Boronat, A. (2002) *Plant Physiol.* **130,** 1079–1089.
3. Wagner, K.-H. & Elmadfa, I. (2003) *Ann. Nutr. Metab.* **47,** 95–106.
4. Qureshi, N. & Porter, W. (1981) in *Biosynthesis of Isoprenoid Compounds*, eds. Porter, J. W. & Spurgeon, S. L. (Wiley, New York), pp. 47–94.
5. Newman, J. D. & Chappell, J. (1999) *Crit. Rev. Biochem. Mol. Biol.* **34,** 95–106.
6. Eisenreich, W., Schwarz, M., Cartayrade, A., Arigoni, D., Zenk, M. H. & Bacher, A. (1998) *Chem. Biol.* **5,** R221–R233.
7. Lichtenthaler, H. K. (1999) *Annu. Rev. Plant Physiol. Plant Mol. Biol.* **50,** 47–65.
8. Rohmer, M. (1999) in *Comprehensive Natural Product Chemistry,* ed. Cane, D. E. (Pergamon, Oxford), pp. 45–68.
9. Piel, J., Donath, J., Bandemer, K. & Boland, W. (1998) *Angew. Chem. Int. Ed.* **37,** 2478–2481.
10. Adam, K. P., Thiel, R. & Zapp, J. (1999) *Arch. Biochem. Biophys.* **369,** 127–132.
11. Jux, A., Gleixner, G. & Boland, W. (2001) *Angew. Chem. Int. Ed.* **40,** 2091–2093.
12. Hemmerlin, A., Hoeffler, J. F., Meyer, O., Tritsch, D., Kagan, I. A., Grosdemange-Billiard, C., Rohmer, M. & Bach, T. J. (2003) *J. Biol. Chem.* **278**, 26666–26676.
13. Laule, O., Furholz, A., Chang, H. S., Zhu, T., Wang, X., Heifetz, P. B., Gruissem, W. & Lange, B. M. (2003) *Proc. Natl. Acad. Sci. USA* **100**, 6866–6871.
14. Schuhr, C. A., Radykewicz, T., Sagner, S., Latzel, C., Zenk, M. H., Arigoni, D., Bacher, A., Rohdich, F. & Eisenreich, W. (2003) *Phytochem. Rev.* **2,** 3–16.
15. Dudareva, N., Martin, D., Kish, C. M., Kolosova, N., Gorenstein, N., Faldt, J., Miller, B. & Bohlmann, J. (2003) *Plant Cell* **15,** 1227–1241.
16. Dudareva, N., Murfitt, L.M., Mann, C. J., Gorenstein, N., Kolosova, N., Kish, C. M., Bonham, C. & Wood, K. (2000) *Plant Cell* **12,** 949–961.
17. Kita, T., Brown, M. S. & Goldstein, J. L. (1980) *J. Clin. Invest.* **66,** 1094–1100.
18. Piel, J. & Boland, W. (1997) *Tetrahedron Lett.* **38,** 6387–6390.
19. Jux, A. & Boland, W. (1999) *Tetrahedron Lett.* **40,** 6913–6314.
20. Donath, J. & Boland, W. (1995) *Phytochemistry* **39,** 785–790.
21. Kolosova, N., Gorenstein, N., Kish, C. M. & Dudareva, N. (2001) *Plant Cell* **13,** 2333–2347.
22. Kuzuyama, T., Shimizu, T., Takahashi, S. & Seto, H. (1998) *Tetrahedron Lett.* **39,** 7913–7916.
23. Bach, T. J. & Lichtenthaler, H. K. (1983) *Physiol. Plant*. **59**, 50–60.
24. Funk, J. L., Jones, C. G., Baker, C. J., Fuller, H. M., Giardina, C. P. & Lerdau, M. T. (2003) *Ecol. Appl.* **13**, 269–278.
25. Arimura, G., Huber, D. P. W. & Bohlmann, J. (2004) *Plant J.* **37,** 603–616.
26. Tholl, D., Kish, C. M., Orlova, I., Sherman, D., Gershenzon, J., Pichersky, E. & Dudareva, N. (2004) *Plant Cell* **16,** 997–992.
27. Estevez, J. M., Cantero, A., Reindl, A., Reichler, S. & Leon, P. (2001) *J. Biol. Chem.* **276,** 22901–22909.
28. Takahashi, S., Kuzuyama, T., Watanabe, H. & Seto, H. (1998) *Proc. Natl. Acad. Sci. USA* **95,** 9879–9884.
29. Julliard, J. H. & Douce, R. (1991) *Proc. Natl. Acad. Sci. USA* **88,** 2042–2045.
30. Himmeldirk, K., Kennedy, I. A., Hill, R. E., Sayer, B. G. & Spenser, I. D. (1996) *Chem. Commun.* **10,** 1187–1188.
31. Bick, J. A. & Lange, B. M. (2003) *Arch. Biochem. Biophys.* **415,** 146–154.
32. Rodriguez-Concepcion, M., Fores, O., Martinez-Garcia, J. F., Gonzalez, V., Phillips, M. A., Ferrer, A. & Boronat, A. (2004) *Plant Cell* **16,** 144–156.
33. McCaskill, D. & Croteau, R. (1995) *Planta* **197,** 49–56.
34. Boucher, Y. & Doolittle, W. F. (2000) *Mol. Microbiol.* **37,** 703–716.
35. Lange, B. M., Rujan, T., Martin, W. & Croteau, R. (2000) *Proc. Natl. Acad. Sci. USA* **97,** 13172–13177.